BEAM DIAGNOSTICS FOR CYCLOTRONS

R. Dölling, Paul Scherrer Institut, Villigen, Switzerland

Abstract

An overview of beam diagnostic systems for cyclotron operation and development is presented. The focus is on devices installed within the cyclotron with its special "environmental" conditions and limitations. Emphasis is placed on the requirements of high current beams, as produced by the PSI Injector 2 and Ring cyclotrons [1].

INTRODUCTION

The first operating cyclotron already used a Faraday cup to detect the accelerated beam current (Fig. 1). Since then, both cyclotrons and beam diagnostic systems have undergone several development cycles, leading to the variety of cyclotrons in operation today at a number of scientific, industrial and medical facilities [2, 3].

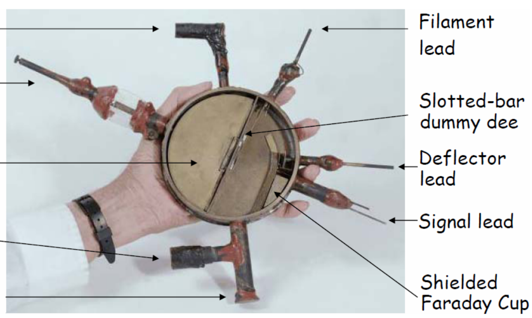

Figure 1: Lawrence & Livingston 4-inch cyclotron which delivered 80 keV protons in 1931 (picture from [4]).

Most of the beam diagnostic techniques in use today at cyclotrons were already present in the 1970s. These are reviewed in [5] and [6-9] and are further described in the proceedings of this conference series (since 1959). In addition, a wealth of detailed information on beam diagnostic techniques is available from the Proceedings of the Beam Instrumentation Workshops (BIW, since 1989) and the Beam Diagnostics and Instrumentation for Particle Accelerators Conferences (DIPAC, since 1993) and other accelerator conferences. Overviews are given in, e.g. [10-14].

Machine design and operation has profited over the years from a number of theoretical and experimental advances. These include improvements in the fields of beam dynamics and magnetic field mapping, and in the stability and reliability of machine components. The experience gained has also played a part. At the same time, requirements to beam quality and availability have also steadily increased. Beam diagnostic systems are thus called on to deliver the missing ε of information during commissioning, beam development, setup and tuning, and searches for anomalies. They are similarly required for beam stabilization and machine protection during standard operation and for the avoidance of excessive activation.

Due to the large variation in cyclotron concepts, uses and parameters, beam diagnostic systems have to adapt to many different environments. Beam current, energy and particle species and their variability, external or internal ion source, sector-focusing or not, separate sectors or compact, normal- or superconducting coils, separated or non-separated turns at extraction as well as standalone or coupled machines, unique or series cyclotron models and the different demands to the availability of the facility - all place their constraints on the requirements.

The boundary conditions within the cyclotron are especially stringent. Already the simultaneous presence of many turns, which eventually overlap, or exhibit beam halo or provide a high power beam, is in itself a complication to the 1-orbit case. The limited space, the strong magnetic field and the presence of large RF fields, beam losses and subsequent radiation, activation and perturbing particles in the direct vicinity of sensor elements, presents a formidable challenge. They hinder or make impossible the use of certain diagnostic techniques and detectors, demanding additional effort. Examples which illustrate this point are shown in Figs. 2, 3.

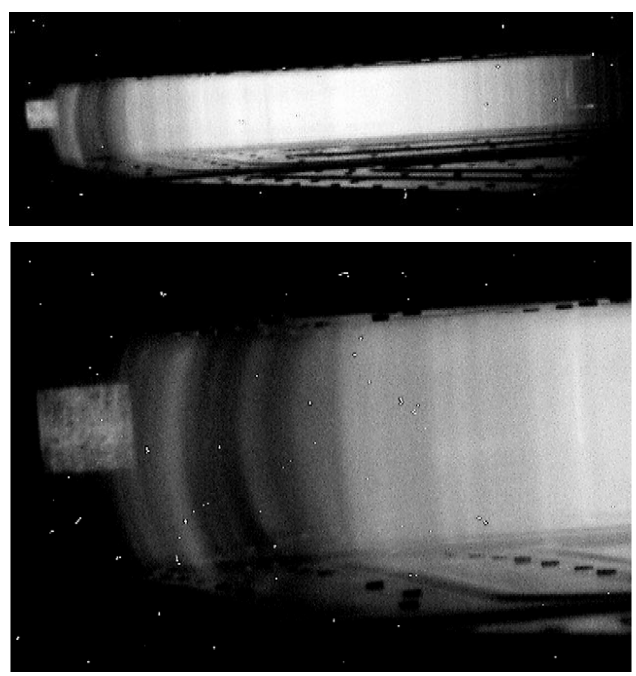

Figure 2: Radial view into the PSI Ring Cyclotron with RF and sector magnets switched on but without beam. A thin plasma is sustained at lower machine radii in the gap of the sector magnet by the RF leaking out from the nearby cavities [15]. One can imagine that the plasma (with associated currents well above the beam current) effects probe measurements.

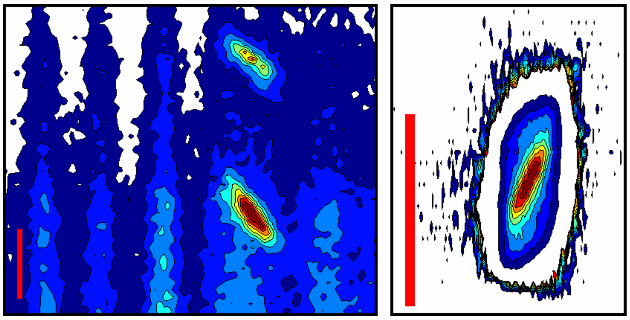

Figure 3: Time-structure measurement of the first two turns in the PSI Ring Cyclotron (left) and of the beam in the injection line (right). Bunches as seen from above move from right to left. The red bars indicate a 1 cm x 1 cm area; contour lines at every 10% (and at the right picture in addition every 10% divided by 125, single event bins are visible). The similar detectors using the same integration time were placed ~0.3 m from the beam. While the measurement in the beam line exhibits mainly shot noise, in the cyclotron a background pattern created by beam losses at other points in the cyclotron significantly decreases the resolution. (The FWHM time resolution of the detector of ~35 ps corresponds to 4 mm [16].) The few centimetres of lead shielding around the detector are not effective against the energetic stray particles.

TASKS

In the cyclotron as well as in the beam lines a fundamental task of beam diagnostics is to deliver information on the beams 6-dimensional (6D) phase space distribution, to the extent that it allows a study of differences in the beam profile/quality to that predicted by beam dynamics simulations ("knowledge aspect"). This involves matching the beam core from the ion source to the injection line, and then into the cyclotron acceptance, the beam path at injection and in the center region where current setting, beam shaping, beam centering and betatron oscillation setting are performed; the isochronism, bunch length and centering in the acceleration region, the beam path through the extraction elements, the matching to the next transport line and the efficiency of transport all along the way.

As a result the settings of magnetic and RF fields and of mechanical elements can be adjusted. Introduced into control loops this improves the beam stability ("stabilization aspect"). Also the sources of beam parameter fluctuations, e.g. magnet power supply ripples, can be traced back. Further important tasks are the prevention of thermal beam damage and the avoidance of excessive activation by monitoring the beam losses and trigger beam abort if necessary ("protection aspect").

At High Current Beams

In the case of high current beams, already a thin beam halo contributes significantly to the beam losses. The transport of the whole distribution is strongly influenced by the beam space charge and the creation of new halo by scattering at collimators. Hence, already small changes at any location along the beam path can alter the total losses strongly. This makes setup and tuning difficult and leads to a tuning method mainly determined by examining the losses of the beam along its path and "turning all available knobs" to minimize losses at a given beam current level [17]. With this concept, the diagnostics serving the "knowledge aspect" are mainly needed to see "what is different than before" in case of unexpected beam behaviour. (The "stabilization aspect" is still needed, e. g. the online beam centering for a ramping up of the beam current within a few seconds.)

Although this empirical concept is useful for finding the optimum operation for a *given* machine configuration, well-directed *changes* of the machine configuration, leading to significant improvement, cannot be initialized by it. Also it is very difficult to find hidden causes in the case of a persistently bad beam quality. To overcome this, detailed numerical simulations [18-20] of the beam transport and matching including the beam halo are required *together* with *detailed* measurements of the 6D phase space distribution. This revitalization of the "knowledge aspect" should result in an improved beam cleaning at low energies by additional slits, a matched beam core *and* halo, lower losses at higher energies, the ability to setup the whole machine in one pass and the ability to find sources of deteriorated beam by examining the beam in detail.

Since the beam transport is strongly determined by space charge, also the "knowledge aspect" diagnostics must be operable at full beam current.

On the simulations side, fitting capabilities must be included in order to find the best fitted *detailed* phase space distribution to a large set of profile and loss data.

UTILIZABLE EFFECTS

An attempt at categorizing the basic effects used by beam diagnostics of hadron beams is given in Table 1. Their use *within* cyclotrons is discussed in the following sections separately for transversal and longitudinal components.

TRANSVERSAL INFORMATION

Collimators and Radial Probes

Segmented aperture foils and fixed or movable collimators use direct current measurement at lower particle energies where the beam or a fraction of it is stopped, while at higher energies only the secondary electrons (SE) emitted from the hit surfaces contribute. They help to guide the beam by defining its path and detect beam loss. Sufficient cooling of these devices is only needed if their cutting into the beam is intended, since the switching off of the beam by interlock generation is fast enough to prevent damage.

Most beam probes as well use direct or SE current measurement. (Nevertheless temperature measurement can be a slow but low-noise alternative.) The thermal

Table 1: Categorization of effects that may be used to extract information from an ion beam. (Examples are given in [24]). Indicated are the dimensions of delivered information, approximate beam current range, whether or not the beam is destroyed, if usage within a cyclotron seems feasible (for the magnetic field separate sectors are assumed) and if realized (as far as the author is aware) and if a usage is compatible with high vacuum requirements.

information 1D: 1D-profile 2D: 2D-profile Dz: long. prof. Pos.: position E: energy C: full current	configuration	usable effect/device	usable A) for machine safety B) permanently C) for tuning D) at setup E) for error search F) only at commiss.	destructive	able to work inside cycl.	alrdy. used inside cycl.	usabl. at good vacui	beam current range (assumed DC beam at 70 MeV, 10 mm diameter, to be determined more precisely)	common names
		beam self fields							
Pos, Dz, C	pickups	comparison of capacitively or inductively coupled RF currents	A B C D E	no	x	**x**	x	nA ... A	pickup, BPM, phase probe
C, (Dz)	transformer	DC or AC current transformer, wall current monitors	A B C D E	no	?		x	nA ... A	DCCT, ACCT, wall curr. m.
1D, C, (Dz)	"wire"	electron (or ion) beam probe	B C D E	no			x	mA ... >A	electron beam probe
1D, C	residual gas	residual gas ions (with beam space charge field)	?	no			(x)	mA ... >A	[21]
		direct beam current							
1D (/+Dz), C	in full beam	probe finger: current of stopped beam fraction (/+50Ω-readout)	D E	yes	x	**x**	x	nA ... uA	radial probe/Faraday cup
<1D	beam edge	collimator: -"-	A B C D	"no"	x	**x**	x	pA ... mA	collimator
1D, C	wire	wire: -"-	C D E	~no	x	**x**	x	-	wire scanner
		heating of introduced solid matter							
1D, C	in full beam	probe finger: direct (or cooling water) temperature measurement	D E	yes	x	x	x	nA ... uA	calorimeter probe
<1D	beam edge	collimator: -"-	B C D	"no"	x	x	x	nA ... mA	
1D, C	wire	vibration resonance shift	C D E	~no	?		x	pA ... uA	vibrating wire scanner
1D	wire	wire: resistance	C D E	~no	x		x	uA ... mA	
E, C	in full beam	probe finger: 2 thermocouples + degrader	C D E	yes	x		x	nA ... mA	[22]
2D, C	in full beam	metal/carbon foil: thermal light emission/thermionic emission	A B F	~yes	x	x	x	uA	[23, 6]
1D	wire	wire: -"-	C D E	~no	x	x	x	uA ... mA	
		changes to introduced solid matter							
2D	in full beam	paper/Kapton/Mylar darkening, metal foil burn	F	yes	x	**x**		nA ... uA	foil burn
2D, C	in full beam	radiochromic film	F	yes	x	**x**		<pA ... nA	
2D, C	in full beam	foil activation analysis, autoradiograph	F	yes	x	**x**	x	pA ... uA	autoradiograph
		secondary particles from introduced solid matter							
1D, C	wire	wire: secondary emission current, direct measurement	C D E	~no	x	**x**	x	pA ... mA	wire scanner
<1D, C	beam edge	foil: -"-	A B C D E	"no"	x	**x**	x	pA ... uA	SEM foil, aperture foil
2D, C	in full beam	foil: secondary emission current + pulling + 2D-electron detector	A B C D E	~no	x		x	pA ... uA	
1D, Dz, C	wire	wire + detection of scattered or secondary particles	C D E	~no	x	**x**	x	nA ... mA	time structure m./wire scanner
Dz, C	in full beam	foil + detection of scattered or secondary particles	C D E	~no	x	**x**	x	nA ... mA	time structure measurement
2D, C	in full beam	scintillating screens + 2D-light detector	C D E	yes	x	**x**	x	pA ... uA	scintillator screen/viewer probe
1D, Dz, C	"wire"	scintillating fibres + (external) PMT	C D E	~no	x		x	<pA ... nA	
Dz, C	in full beam	scintillator + (external) PMT	C D E	yes	x	x	x	<pA	time structure measurement
<=2D,Dz,E,C	in full beam	silicon/diamond bulk/strip/pixel detector	C D E	yes	x	x	x	<pA/<nA	silicon strip detector
		secondary particles from introduced dense gases							
1D, C	"wire"	coaxial ionisation chamber	C D E	~yes	x		x	<pA ... uA	
1D, C	in full beam	ionisation chamber + strip-electrode readout (in beam/not)	(B) C D E	yes/~yes	x		x	<pA ... uA	strip ionisation chamber
2D, C	in full beam	ionisation chamber + pixel-electrode readout (in beam)	C D E	yes	x		x	<pA ... uA	pixel ionisation chamber
1D	in full beam	proportional chamber	C D E	~yes			x	<<pA ... nA	wire chamber
1D, 2D, C	in full beam	GEM	C D E	yes	x?		x	<<pA ... nA	GEM
		secondary particles from residual or thin gas							
2D, C	gas curtain	beam induced fluorescence + (external) light detector	A B C D E	~no				nA ... >A	gas curtain
1D, C	residual gas	beam induced fluorescence + (external) light detector	A B C D E	no	x	x	(x)	mA ... >A	BIF monitor
1D (2D), C	residual gas	res. gas ions/electrons with external fields + strip(/+energy) det.	A B C D E	~no	x	x		uA ... A	residual gas profile monitor

beam load sets limits to the use of any solid material placed in the beam. Thin carbon fibres are most resistant at higher particle energies (where the stopping power is lower and the particles pass the wire) while water-cooled tilted copper or carbon surfaces tolerate the highest beam power densities at low energies. In between can be a gap where only non-destructive methods are applicable with high current beams, in order not to be thermally damaged and to limit the activation by induced beam losses.

Different types of radial probe heads are depicted in Fig. 4. Integral probes A - D provide the beam current depending on radial position by fully stopping the beam in the thick electrodes. Differential probes C - H yield the radial beam current density. Probes B, C, G, H, I give information on the axial distribution by segmentation [7, 25] and F by a rough tomography [26]. At the thick probes A - D the radius-defining face-side must be aligned tangential to the beam direction to minimise the amount of scattered particles and protruding axial end-caps (not shown) are added to catch SE spiralling along the axial magnetic field lines. Ideally these measures should result in a probe efficiency near to 1, but this is often not the case. At probes G, I the interference of SE from different vertical segments have to be prevented by lateral off-set. In some instances the electrodes are biased or electrodes have been added for pulling away the SE [27, 7, 26]. RF fields and stray particles (as SE or residual gas ions or scattered or secondary beam particles) often disturb the measurements. A closed shielding is only possible at low beam current and at the expense of losing information at the lowest energies, and is seldom used [28].

Radial probes are used for beam centering and provide information on radial and axial coherent and incoherent betatron oscillation amplitude and frequency [5].

Thick probes are convenient tools for "pulling" the beam to larger radii at low current and directly indicate current losses. If the turns are not separated, the "shadow width" of the exchange of signal from a fixed integral probe to a moving integral probe at a different azimuth provides information on the amplitude of the incoherent radial betatron oscillation and the radial turn profile [29, 30]. The cross-over radii of both probes must be equalized for centering ("50% method" [31]). At separated turns, the radial information is more easily obtained by differential probes.

In high current beams above ~20 MeV, (if at all) only the thin probes E, F survive. They also have the added advantage that the increase to beam loss is only moderate.

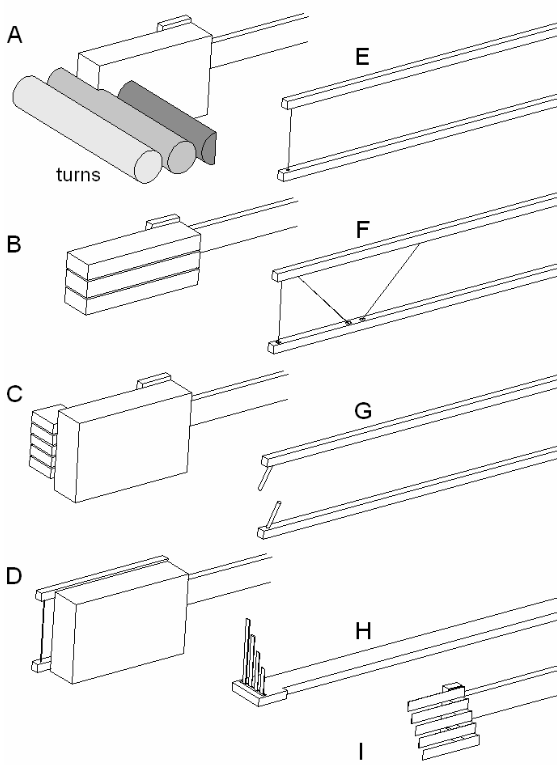

Figure 4: Schematic view of different radial probe heads.

Non-Destructive Profile Measurement

The effort for fully or nearly non-destructive methods seems only justifiable in the case of high power beams. Secondary emission monitors and residual gas ion monitors [32], which in certain configurations can deliver 2D transversal profiles [33, 34], have only occasionally been used within cyclotrons in 1D configuration [35, 36], using the cyclotron magnetic field for particle guidance, an electric pulling field and simple collecting electrodes. (In beam lines usually detectors with inherent amplification are used, but sensitivity is not an issue here and furthermore many detectors, e.g. the multichannelplate, are not usable in high magnetic fields.)

Beam-induced fluorescence profile monitors [37, 38] are in use at the 0.87 MeV injection line to the Injector 2 cyclotron at PSI [26], and may be suitably used to provide a radial profile of the inner turns in the cyclotron, which are not accessible at full beam current to the radial wire probes. Intensified CCD cameras may not be sufficiently radiation hard. Photomultiplier tubes [26, 38] can be a candidate because of their sensitivity, low noise and radiation hardness, but must be magnetically shielded (which is only possible in separate sector cyclotrons) or a relay optic must be used to transfer the image to the outside. Nevertheless the impact of stray light from perturbing effects (see Fig. 2) is not clear. In any case it will limit the dynamic range to less than ~1000.

Halo Measurement

More detailed measurements of the beam halo are of great interest for the understanding of the transport and beam losses of high current beams. With thin wire probes it is difficult to achieve the required dynamic range (of the order of 10^5 for a projected profile in the PSI facility) in the environment of the cyclotron and with the above mentioned non-destructive methods this seems even less promising. Therefore the halo should be measured separately from the beam core by moving an axial probe finger radially and axially as far as the probe heating allows. Encapsulated in the finger, a current or temperature measurement or, more sensitive, a small ionisation chamber or diamond detector [39] could provide a very large dynamic range since being shielded against RF fields and low energy stray particles.

The same technique could also be applied to beam lines by moving a finger or slit transversely into the beam. At higher energies also wire monitors with direct current measurement or detection of scattered particles seem feasible [40]. (In the 72-MeV injection line to the PSI ring cyclotron, the present thin-wire scanners are read out with logarithmic amplifiers which have a dynamic range from 50 pA to 1 mA. Nevertheless, their bandwidth at low current is too low and hence changes in the beam profile are indeed visible down to 10^{-5} levels of the maximum signal, but the local signal depends also heavily on the signal history below a 10^{-3} level.)

Image-Based Methods

For commissioning, techniques such as foil burning [6, 41] or autoradiographs, which deliver a 2D profile, are often used. They allow for the initial adjustments of the magnetic field at a minimum cost, but require the machine to be opened several times. More convenient are viewer probes which insert a scintillator screen into the beam, an image of which is recorded by an internal or external camera [42].

Very Low Current Beams

In most machines the setup is usually done with an initially low beam current, still giving sufficient signal, but limited activation. The beam current is then increased to the operation level. On the opposite for very low current radioactive ion beams an already low current pilot beam of nearly equal charge to mass ratio is used to get sufficient signal from essential monitors, before using the particle species of interest. Here sensors with inherent amplification are placed directly into the beam [14, 43].

PHASE AND TIME-STRUCTURE

The measurement of the "phase history", the radial dependency of the beam center phase with respect to the RF in the radial or spiral acceleration gap, allows to control the isochronism of the bunches and to adjust main field and trimcoils or trimrods accordingly.

The Garren-Smith method [29] measures the dependence of the bunch center phase and phase width on the orbit radius by detuning the amplitude of the main magnetic field or the RF frequency until both the phase shift at the location of the radial probe reaches ±90° and the probe current decreases. This method is still widely in use for low current beams.

Phase probes, formed by pairs of pickups above and below the midplane coupling capacitively to the beam, can detect the bunch center phase with high accuracy. Usually ~10 probes are arranged along a machine radius, each covering several turns, but also a single radially movable probe is often used. To suppress beam unrelated RF, the probes are operated at higher harmonics or a synchronous detection of a purposely introduced modulation of the beam is used [44]. Usually both pickups of a pair are directly connected, thereby relinquishing the vertical position information. Also the time-structure of the beam can be measured with phase probes, but the resolution is limited due to the longitudinal extensions of beam self fields and pickup.

From the turn numbers dependence on radius one can determine the radial distribution of the accelerating gap voltage. With phase probes the time-of-flight through the cyclotron (or up to a certain radius [44]) can be determined, using cross-correlation and making use of a lower-frequency pulse structure [25] or the beam noise provided by the ion source [45]. This gives the number of turns in the cyclotron even when the turns are not separated.

Time-structure probes are an alternative to phase probes. At low beam currents a thick radial probe is placed in the beam, while at high beam currents a thin wire or foil is introduced and the arrival time of scattered beam particles, gammas or secondary electrons is measured by an internal or external detector with respect to the RF reference phase, e.g. multi-channel plates [46], diamond detectors [47] or scintillator-photomultiplier combinations [16] can be used as detectors. The target precisely defines the location of measurement and hence the time-structure even of short bunches can be determined with good accuracy. Although the pulse width from scintillator and photomultiplier is quite large (~2 ns), its time-resolution can be excellent due to the statistics from the many created photo-electrons. However, the level of radiation background from beam losses strongly determines the resolution and dynamic range (Fig. 3)

Using a wire target has the additional advantage, that a transversal coordinate is also determined. By moving the wire, a 2D profile can be measured (Fig. 3). Repeating this with several wire orientations, does not yield the full 3D spatial charge density distribution, but rather several 2D-projections. Hence e.g. all 9 parameters describing size and orientation of an ellipsoid representing the bunch can be determined and used in beam transport simulations. This type of measurement is under preparation for the PSI Injector 2 cyclotron, the connection beam line to the Ring cyclotron and its extraction line.

While time-structure probes need to sample over many seconds, gridded Faraday cups in 50 Ω-geometry [48] or a strip-line passed by the beam [49] can deliver the time-structure of single bunches, but are destructive.

PARTICLE ENERGY

In beam lines, beam energy and energy spread are usually determined using spectrometers, time-of-flight measurements, scattering or degrading methods. If in a cyclotron several particle species of similar charge to mass ratio are accelerated simultaneously, their separation by the cyclotron can be observed with a time-structure measurement. If the mass resolution of the cyclotron is not sufficient for a separation, the presence of different particles can still be detected by a measurement of their energy or stopping power with a thick or thin solid-state detector. The energy spread is thereby also measured. For low current beams this has been done by placing the detector directly into the beam [43].

EMITTANCE

Emittance measurements deliver start and check point information for beam transport simulations. In beam lines, the beam emittance can be determined by several direct (slit-slit, pepperpot and derived methods as e. g. Allison-scanner [50]) and indirect methods (quadrupole variation with 1 profile monitor behind, 3 profile monitors at different places without focussing in between, beam transport simulation fit to many profile monitors), with the latter suitable for high current beams.

Within the cyclotron [51] or a test stand simulating its center [52] the transversal emittance of an internal ion source has been measured directly although the limited space makes this difficult. At high beam currents, one could think of something similar for the beam halo, but for the beam core only the transport fit to radial or vertical profiles of many turns remains. Nevertheless, since beam width and angular distribution are coupled via the incoherent betatron oscillation, the emittance can also be approximately derived from beam width, orbit radius and betatron frequency.

BEAM LOSS

Collimator and aperture-foil current readings and the less sensitive comparison of full current measurements ("transmission measurement") almost directly determine beam losses. In addition, at not too low beam energies, beam losses are measured by detecting scattered beam particles or secondary particles. A variety of loss monitors are used mostly outside of the machine vacuum [53, 54].

A calibration of the sensitivity of these monitors can be established by deliberately steering a low current beam into the vacuum chamber at several locations [55]. This gives only a rough estimate, because it strongly depends on the relative position of loss and detector. Summing up the signal currents for larger machine sections, weighted also for beam energy, gives the operators an approximate but fast indication of machine performance concerning loss, activation and skyshine [56].

At PSI simple ionisation chambers filled with ambient air are in use since decades. The response is linear up to all dose rate levels of interest [57] and at excessive losses the beam is switched off by the machine-protection system in the order of a millisecond.

Profiles measured by detecting externally the loss induced by a radial probe may be distorted due to the fact that particles, which are scattered at different parts of the probe head or at different probe positions, can be stopped at different places depending on the actual cyclotron geometry. On the other hand, losses caused purposely at known positions, e.g. from wire scanners or wire probes, can provide a cross-check for beam dynamic simulations.

CONCLUSION

Although it has been possible to measure almost any beam property of interest since many years [5], uncertainties in the beam behaviour and the beam halo nevertheless exist. Empirical tuning thus remains essential in establishing and optimizing the beam. The continued efforts in bettering beam dynamic simulations together with beam diagnostic systems will further increase our understanding of beam behaviour, ultimately alleviating the overdependence on empirical tuning. This will consequently lead to an improved machine performance, and will also suggest improvements in equipment and modes of operation or even completely new facilities.

ACKNOWLEDGEMENTS

The Author would like to thank PSI colleagues for useful discussions and M. Rohrer for the CAD drawing.

REFERENCES

[1] M. Seidel et al., "Production of a 1.3 MW Proton Beam at PSI", IPAC10, p. 1309.
[2] J.R. Richardson, "A Short Anecdotal History of the Cyclotron", CYC84, p.617.
[3] M.K. Craddock et al., "Cyclotrons and Fixed-Field Alternating-Gradient Accelerators", Rev. Acc. Sci. Tech. 1, p. 65 (2008).
[4] M.K. Craddock, Lecture "Introduction to Particle Accelerators", http://trshare.triumf.ca/~craddock/PH555/Intro-1.pdf.
[5] G.H. Mackenzie, "Beam Diagnostic Techniques for Cyclotrons and Beam Lines", CYC78, p. 2312.
[6] D.J. Clark, "Beam Diagnostics and Instrumentation", CYC66, p. 15.
[7] M. Olivo, "Beam Diagnostics Equipment for Cyclotrons", CYC75, p. 331.
[8] B. Launé, "Diagnostics for Radioactive Beams", CYC01, p. 359.
[9] J. Dietrich, "Recent Beam Diagnostic Techniques", CYC95, p. 186.
[10] P. Forck, "Lecture Notes on Beam Instrumentation and Diagnostics", JUAS 2010, http://www-bd.gsi.de/conf/juas /juas_script.pdf.
[11] U. Raich, "Instrumentation in small, low energy machines", DIPAC05, p. 1.
[12] P. Strehl, "Beam Instrumentation and Diagnostics", Springer 2006, ISBN 978-3-540-26401-9.
[13] Contributions to several CERN Accelerator Schools (CAS): e. g. many authors at CAS2008 Dourdan; R. Jones, H. Schmickler, K. Wittenburg at CAS2007 Daresbury; U. Raich at CAS2006 Zakopane; H. Koziol at CAS2000 Loutraki; http://cas.web.cern.ch.
[14] V.A. Verzilov, "Progress with Low Intensity Diagnostics at ISAC", IPAC10, p. 885.
[15] Picture from R. Kan, PSI. See also M. Humbel et al., "Disturbance Effects Caused by RF Power Leaking Out from Cavities in the PSI Ring Cyclotron", this conference.
[16] R. Dölling, "Measurement of the Time-Structure of the 72-MeV Proton Beam in the PSI Injector-2 Cyclotron", DIPAC01, p. 111.
[17] T. Stammbach, "Experience with the High Current Operation of the PSI Cyclotron Facility", CYC92, p. 28.
[18] A. Adelmann et al., "On Start to End Simulation and Modeling Issues of the Megawatt Proton Beam Facility at PSI", PAC05, p. 3319.
[19] J.J. Yang et al., "Beam Dynamics in High Intensity Cyclotrons Including Neighboring Bunch Effects: Model, Implementation, and Application", Phys. Rev. ST Accel. Beams 13, 064201 (2010).
[20] Y.J. Bi et al., "Towards Quantitative Predictions of High Power Cyclotrons", this conference.
[21] R. Dölling, "Determination of Radial Ion Beam Profile from the Energy Spectrum of Residual Gas Ions Accelerated in the Beam Potential", DIPAC99, p. 50.
[22] E. Bollmann et al., "A Simple Probe for the Relative Measurement of Beam Energies", CYC84, p. 419.
[23] H.G. Blosser, "Beam Quality Measurements and Focusing Grid Studies", CYC59, p. 203.
[24] R. Dölling, "Beam Diagnostics for Cyclotrons", Educational Session, ECPM XXXVII, Groningen, 2009. http://www.kvi.nl/~agorcalc/ECPM2009/EducationalSession/4_Doelling.pdf
[25] M.K. Craddock et al., "Properties of the TRIUMF Cyclotron Beam", CYC75, p. 240.
[26] L. Rezzonico, "Beam Diagnostics at SIN", CYC86, p. 457.
[27] W.R. Rawnsley, "A Current Mirror Circuit to Bias Beam Intercepting Pick Up Electrodes", TRI-DN-90-14, TRIUMF (1990).
[28] D.J. Clark et al., "Design and Operation of the U.C.L.A. 50 MeV Spiral-Ridge Cyclotron", CYC62, p. 1.
[29] A.A. Garren, L. Smith, "Diagnosis and Correction of Beam Behavior in an Isochronous Cyclotron", CYC63, p. 18.
[30] Y.N. Rao et al., "Calculations on LE2 Probe Head Thickness and Experimental Measurements", TRI-DN-04-8, TRIUMF (2004).
[31] H.W. Schreuder, "Shadow Measurements in a Cyclotron", NIM 95 p. 237 (1971).
[32] P. Forck, "Minimal Invasive Beam Profile Monitors for High Intense Hadron Beams", IPAC10, p. 1261.
[33] L. Badano et al., "A Real-Time Beam Monitor for Hadrontherapy Applications Based on Thin Foil Secondary Emission and a Back-Thinned Monolithic Pixel Sensor", DIPAC07, p. 352.
[34] M. Poggi et al., "Two-Dimensional Ionization Beam Profile Measurement", DIPAC09, p. 384.
[35] B. W. Allardyce et al.. "The Use of a Secondary Emission Monitor in the Extraction Channel of the CERN Synchro-Cyclotron", CYC75, p. 355.
[36] Z.B. du Toit et al., "Operating Experience with the Light-Ion Injector of the NAC", CYC86, p. 109.
[37] F. Becker et al., "Beam Induced Fluorescence Monitor & Imaging Spectrography of Different Working Gases", DIPAC09, p. 161.
[38] J. Dietrich et al., "Non-Destructive Beam Position and Profile Measurements Using Light Emitted by Residual Gas in a Cyclotron Beam Line", EPAC08, p. 1095.
[39] E. Griesmayer et al., "Diamond Detectors as Beam Monitors", BIW10.

[40] K. Wittenburg, "Halo and Bunch Purity Monitoring", CAS2008.
[41] W.C. Parkinson et al., "Modifications to the University of Michigan 83-Inch Cyclotron to Improve Beam Quality", CYC72, p. 366.
[42] F. Marti et al., "Internal Beam Dynamics Studies with a TV Probe", CYC92, p. 435.
[43] F. Chautard et al., "GANIL Status Report", EPAC04, p. 1270.
[44] T.W. Nijboer et al., "Beam-Phase Measurement in the AGOR-Cyclotron", CYC04, p. 416.
[45] F. Loyer et al, "New Beam Diagnostics at GANIL: Very Sensitive Current Transformers in Beam Lines and Counting System of Beam Turns in Cyclotrons", PAC85, p. 1938.
[46] W.R. Rawnsley et al., "The Production and Measurement of 150 ps Beam Pulses from the TRIUMF Cyclotron", CYC84, p. 237.
[47] T. Milosic et al., "Longitudinal Emittance Measurement Using Particle Detectors", DIPAC09, p. 330.
[48] F. Loyer et al, "Main Beam Diagnostics at GANIL", CYC81, p. 585.
[49] V. Verzilov et al., "A Wideband Intercepting Probe for the TRIUMF Cyclotron", TRI-DN-06-1, TRIUMF (2006).
[50] H.R. Kremers et al., "Comparison Between an Allison Scanner and the KVI-4D Emittance Meter", ECRIS08, p. 204.
[51] A.A. Arzumanov et al., "Alteration of the Ion Beam Emittance on the First Orbits in the Cyclotron", CYC81, p. 469.
[52] E.R. Forringer, "Phase Space Characterization of an Internal Ion Source for Cyclotrons", Dissertation 2004, MSU.
[53] K. Wittenburg, "Beam Loss Monitors", CAS2008.
[54] L. Fröhlich, "Beam Loss Monitors", ERL Instrumentation Workshop, Cornell Univ., 2008, http://tesla.desy.de/~lfroehli/download/ERL_instrumentation_ws_2008_BLMs.pdf
[55] U. Schryber et al., "High Power Operation of the PSI-Accelerators", CYC95, p. 32.
[56] W. Joho, "Recent and Future Developments at S.I.N.", CYC78, p. 1950.
[57] R. Dölling et al., "Beam Diagnostics at the High Power Proton Beam Lines and Targets at PSI", DIPAC05, p. 228.